Eur. Phys. J. B **46**, 471–474 (2005)
DOI: 10.1140/epjb/e2005-00276-2

THE EUROPEAN
PHYSICAL JOURNAL B

# Synthesis and magnetic properties of $FeNi_3/Al_2O_3$ core-shell nanocomposites

W. Liu, W. Zhong[a], H.Y. Jiang, N.J. Tang, X.L. Wu, and W.Y. Du

National Laboratory of Solid State Microstructures, Physics Department, Nanjing University, Nanjing 210093, P.R. China

Received 14 January 2005 / Received in final form 21 May 2005

**Abstract.** In this study, $FeNi_3/Al_2O_3$ core-shell nanocomposites, where individual $FeNi_3$ nanoparticles were coated with a thin layer of alumina, were fabricated by a modified sol-gel method. Several physical characterizations were performed on the samples of $FeNi_3/Al_2O_3$ nanocomposites with different thickness of $Al_2O_3$ shell. The encapsulation of $FeNi_3$ nanoparticles with alumina stops $FeNi_3$ agglomeration during heat treatment, and prevents interaction among the closely spaced magnetic $FeNi_3$ nanoparticles. The $Al_2O_3$ insulating shell improves the soft magnetic properties of $FeNi_3$. The study of the complex permeability of the samples shows that the real part $\mu'$ of the permeability of the sample with Al molar content of 20% (Al/(Fe+Ni)) is as high as 12, and independent of frequency up to at least 1 GHz. The tunneling magnetoresistance arising from the presence of the $Al_2O_3$ shell have also been studied.

**PACS.** 75.50.Bb Fe and its alloys – 75.75.+a Magnetic properties of nanostructures – 81.07.-b Nanoscale materials and structures: fabrication and characterization

## 1 Introduction

Magnetic nanocomposites, consisting of magnetic metal nanoparticles coated with a nonmagnetic insulator (e.g., polymer, alumina, or silica), have attracted particular attention due to their potential uses as microwave absorbing and shielding materials [1] as well as their applications in electromagnetic devices [2]. For example, nanocomposites with soft magnetic properties can be incorporated in high-frequency devices and in micro-transductors which require large magnetic moment and susceptibility, low coercivity, and high resistivity [3–5]. FeNi alloy is a well-known and commonly used soft magnetic material. However, due to the intrinsic property of the metal particles, the generation of eddy current severely limits its application at high frequency. A strategy to solve the problem is to cover the soft magnetic metallic nanoparticles by an inorganic and non-magnetic coating to create the core-shell nanostructure. This core-shell structure maintains the magnetic properties of metal and its alloys. And better performance can be achieved at high frequency when an insulating shell is applied. Recently, the magnetic and high-frequency properties of FeNi and other Fe-alloy nanocomposites with different insulator matrixes [6–9] have been reported. However, only a few are devoted to $Al_2O_3$-based nanocomposites, and most are related to magnetic metals or alloys embedded in insulator matrixes which were not core-shell structures. Alumina is an effective material to form good barrier for spin-polarized tunnel [10]. The magnetic nanoparticles with alumina shell would result in favorable magnetic properties that could be manipulated by controlling the thickness of the alumina shell. Also, by coating FeNi particles with alumina, one can increase the resistivity and hence reduce losses due to eddy currents. In this paper, we have successfully engineered a modified sol-gel approach to fabricate $Al_2O_3$-coated $FeNi_3$ nanoparticles. The method we used is effective and the process is easy to control. We have also investigated the influences of alumina thickness on the magnetic and transport properties of $FeNi_3$ nanoparticles.

## 2 Experimental

Analytical grade reagents ferrous chloride ($FeCl_2{\cdot}4H_2O$), anhydrous aluminum chloride ($AlCl_3$), nickel chloride ($NiCl_2{\cdot}6H_2O$), citric acid monohydrate and ethanol absolute were used. The thickness of $Al_2O_3$ shell was controlled by the molar percentage of aluminum with respect to the total content of Fe and Ni. The total aluminum contents in the final as-prepared composites were 0%, 4%, 8% and 20% (Al/(Fe+Ni) molar ratio), and the corresponding samples are denoted as $FeNi_3/Al_2O_3$-0, $FeNi_3/Al_2O_3$-4, $FeNi_3/Al_2O_3$-8, and $FeNi_3/Al_2O_3$-20 hereafter. In a typical experiment, 0.01 mol $FeCl_2{\cdot}4H_2O$, 0.03 mol $NiCl_2{\cdot}6H_2O$ and 0.09 mol citric acid monohydrate were dissolved in 100 ml ethanol. After stirring at 60 °C for 6 h, a clear sol was obtained. Then 0.0016 mol $AlCl_3$ was added to the sol and the mixture was stirred for 4 h. After drying the sol at 80 °C, the xerogel was calcinated in air

---

[a] e-mail: wzhong@netra.nju.edu.cn

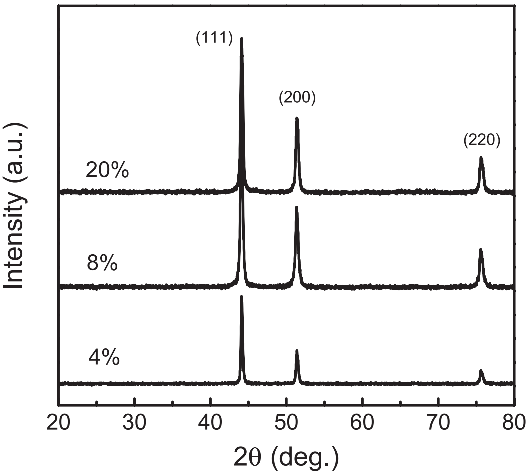

**Fig. 1.** X-ray diffraction patterns of $FeNi_3/Al_2O_3$ nanocomposites with different contents of Al.

at 400 °C for 3 h, followed by reduction at 800 °C in a hydrogen stream of 2 L/h for 4 h. Then the sample with 4 mol% Al/(Fe+Ni) (i.e. $FeNi_3/Al_2O_3$-4) was obtained.

The phase identification and structure analysis of the as-prepared powder samples were characterized by X-ray powder diffraction (XRD) with Cu-K$\alpha$ radiation (Model D/Max-RA, Rigaku, Japan). The morphology of the samples was observed via transmission election microscopy (TEM) (Model JEM-200 CX, JEOL, Japan). The magnetic property was measured by a vibrating sample magnetometer (VSM) (Lakeshore, USA). For complex permeability and magnetoresistance measurements, the powder samples were pressed into a ring and a flake, respectively. Complex permeability spectra were measured with an impedance analyzer (Agilent4284A from 20 Hz to 1 MHz) and an impedance/material analyzer (Agilent4191B from 1 MHz to 1.8 GHz). The magnetoresistance measurement was conducted by the standard four-point method.

## 3 Results and discussion

The XRD patterns of three samples with different contents of Al are shown in Figure 1. The diffraction patterns of the three samples match well with the cubic structure of $FeNi_3$. There are no detectable peaks of metallic iron and nickel or their oxides. The results indicate the successful formation of the $FeNi_3$ alloy. It should also be noted that there is no evidence for the presence of crystalline $Al_2O_3$ either in the XRD patterns or in the electron diffraction patterns for all the samples. As a result, we deduce that the alumina in the $FeNi_3/Al_2O_3$ composites is in an amorphous state.

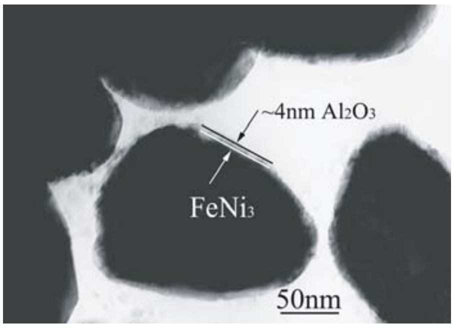

**Fig. 2.** TEM image of the nanoparticles of $FeNi_3/Al_2O_3$-8.

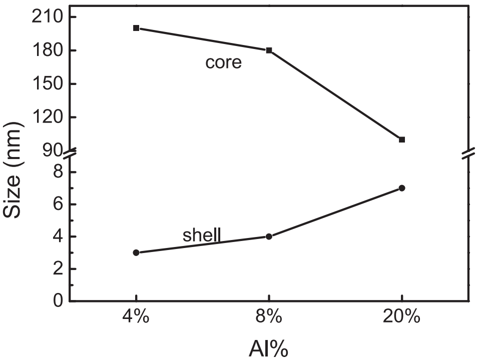

**Fig. 3.** Average grain size of $FeNi_3$ core and thickness of alumina shell as a function of Al molar concentration.

A typical TEM micrograph of the $FeNi_3/Al_2O_3$ nanocomposites with Al molar ratio of 8% is shown in Figure 2. The interface between the $FeNi_3$ cores and the $Al_2O_3$ shell can be observed clearly with high contrast. As indicated, the alumina shell is about 4 nm in thickness. The TEM image demonstrates that the core-shell nanocomposites of $FeNi_3/Al_2O_3$ have been successfully fabricated by the simple chemical method.

The molar ratio between Fe and Al ions was found to be an important parameter for the determination of the size of the $FeNi_3$ core. As shown in Figure 3, the thickness of the alumina shell increases with increasing aluminum content. After reduction at the same temperature, the $FeNi_3$ particles with thicker alumina shell are obviously smaller in size than those with thinner alumina shell. This indicates that the $Al_2O_3$ coating could hinder the agglomeration of the $FeNi_3$ nanoparticles to a certain extent.

The magnetic hysteresis loops at room temperature of the nanoparticles are shown in Figure 4. They are typical hysteresis loops of soft magnetic materials. It should be stressed that the magnetization is expressed in units of emu per gram of powder, with the mass of the nonmagnetic shell being included. Using the molar percentage of the $FeNi_3$ cores in the nanocomposites, the magnetizations of $FeNi_3$ cores were derived. It was found that they were close to the value of $FeNi_3$ alloy without alumina layer. The alumina shell also has an effect on the coercivity of the $FeNi_3$ core. As shown in the inset of Figure 4, the coercivity increases obviously after the $FeNi_3$ particles were coated with alumina, and the coercivity increases slightly with increase in alumina content. As pointed out before, at equal synthesis temperature, the size of $FeNi_3$ particles with thicker $Al_2O_3$ coating was smaller than that with the thinner coating. It's known that the coercivity increases with decreasing grain size for multidomain particles [11],

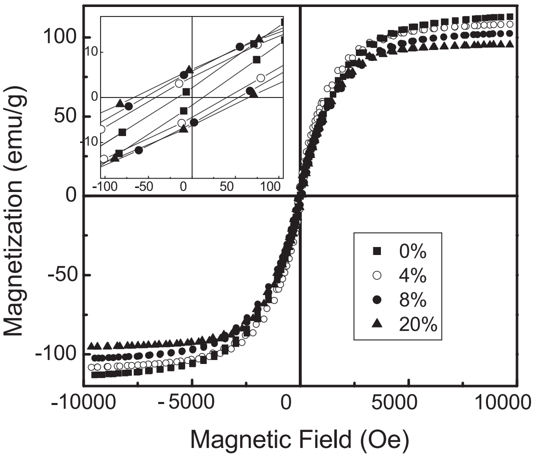

**Fig. 4.** Hysteresis loops for samples with different thickness of $Al_2O_3$ shell. The inset on the top left corner represents the influence of the $Al_2O_3$ shell thickness on the coercivity of $Al_2O_3$-coated $FeNi_3$ nanoparticles.

so it is reasonable to observe that smaller $FeNi_3$ nanoparticles exhibited higher coercivity. The change in $H_C$ values in the alumina-coated samples confirms that the alumina coating is essential to avoid sintering of the $FeNi_3$ particles.

The frequency dependence of the complex permeability for all the samples is shown in Figure 5. It is observed that the real part of permeability. $\mu'$ of the uncoated sample decreased rapidly at 1 MHz. When the alloy was coated by alumina, the cut-off frequency increases obviously. For the sample of $FeNi_3/Al_2O_3$-20, $\mu'$ is independent of frequency up to at least 1 GHz. It is clear that the insulating $Al_2O_3$ shell improves the performance of the soft magnetic $FeNi_3$ cores at high frequency. The performance of conventional soft magnetic materials is strongly dependent on the operating frequency. For metallic magnetic materials, the low cut-off frequency is usually attributed to the eddy currents arising from poor insulation between particles. These currents can lead to significant losses when the applied field is alternating current (AC), particularly at high frequency, and can cause significant heating of the material. If there is no insulated shell, direct metal contact would lead to eddy current, which would cause $\mu'$ to decrease fast with frequency and the imaginary part $\mu''$ reach a maximum at a lower frequency. But in the $Al_2O_3$-coated $FeNi_3$ structure, such limitations could be eliminated. As shown in Figure 5, with the increase in alumina content, the shell thickens and is compact enough for efficient insulation. The thickening of the $Al_2O_3$ coating enhances the resistivity of materials, consequently reducing the effect of eddy currents at high frequency as well as keeping the $\mu'$ almost constant and the imaginary part very small.

In magnetic nanoparticles, coupling between particles can be induced through direct exchange coupling and dipolar interaction. The former is the main way to improve the soft magnetic properties in permeability [6]. In the $FeNi_3/Al_2O_3$ nanocomposites, the dipolar interaction is the main effect because the magnetic particles are well separated by the alumina coating, and exchange interactions are negligible. That is the reason why the $\mu'$ is not very high. On the other hand, compared with the sintered one, the pressed ring is lower in density. The possible reason could be that the nonmagnetic impurities such as boundaries and cavities from the low density may play an important role and may cause further decline in permeability. In other words, the permeability can be significantly improved by manipulating the coating thickness and the density.

$Al_2O_3$ is an effective material to form good barrier for spin-polarized tunneling [10]. Since there is insulating alumina shell between the $FeNi_3$ particles, they may exhibit similar magneto-transport property as that in Ferromagnetic/Insulator/Ferromagnetic (FM/I/FM) tunnel junction, which exhibits tunneling magnetoresistance (TMR) effect. We conducted magnetoresistance measurements for the $FeNi_3/Al_2O_3$-8 and $FeNi_3/Al_2O_3$-20 samples at room temperature and 4 K, respectively. Resistance at zero field ($R_0$) was used as the reference when calculating MR percentage, and detailed investigation was performed between ±12kOe (corresponding resistance is denoted by $R_H$). Figure 6 shows the resistance ratio [MR ratio $= (R_H - R_0)/R_0$] versus magnetic field curve. For the $FeNi_3/Al_2O_3$-8 and $FeNi_3/Al_2O_3$-20 samples, the magnetoresistance ratios were 0.6%, 1.1% at room temperature and 1.0%, 2.1% at 4 K, respectively. It has been pointed out that tunneling magnetoresistance is related intimately with the microstructure of the nanocomposite, such as the grain size, shape, size distribution, and the insulating shell structure [12,13]. If the coating is too thin, the cores of the particles can be in direct contact, leading to short circuit and decrease in tunneling effect; as a result, TMR is lower. This observation is in consistent with the results of the complex permeability measurements. At lower field over our samples, we found the little positive magnetoresistance effect which may be caused by anisotropic magnetoresistance (AMR) of $FeNi_3$ cores. Since Fe-Ni alloy has positive AMR at room temperature and its saturation field is low, TMR of the $FeNi_3/Al_2O_3$ nanocomposites cannot compare with AMR at the low field. However at higher field, the TMR of $FeNi_3$ increased and exceeded the AMR.

## 4 Conclusions

In summary, we have devised a simple chemical method for the synthesis of magnetic $FeNi_3$ nanoparticles that are enclosed by an alumina shell. The surface alumina layer prevents interaction between the closely spaced magnetic $FeNi_3$ particles and hinders grain growth and agglomeration during heat treatment. There is a decrease in $M_S$ and increase in $H_C$ with the increase of the $Al_2O_3/FeNi_3$ ratio. Moreover, $Al_2O_3$ insulating shell improves the soft magnetic properties of $FeNi_3$ alloy. We could obtain soft magnetic nanoparticles with different cut-off frequency by controlling the thickness of the alumina shell. The study of complex permeability of the samples shows that the real part $\mu'$ of the permeability of the sample with Al molar

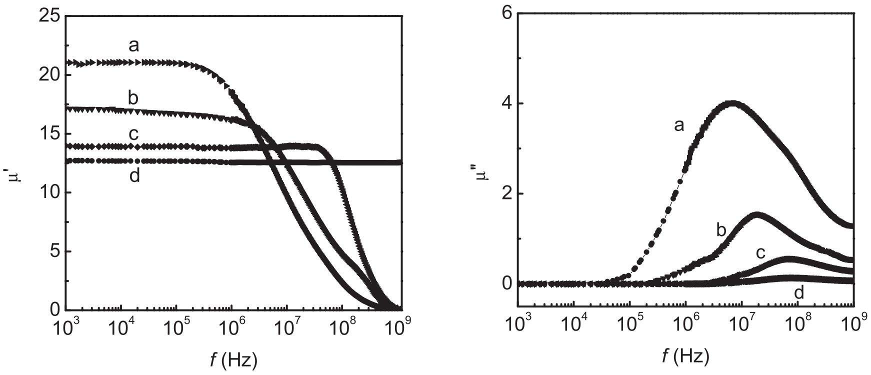

**Fig. 5.** The permeability spectra of the samples: (a) $FeNi_3/Al_2O_3$-0, (b) $FeNi_3/Al_2O_3$-4, (c) $FeNi_3/Al_2O_3$-8, and (d) $FeNi_3/Al_2O_3$-20.

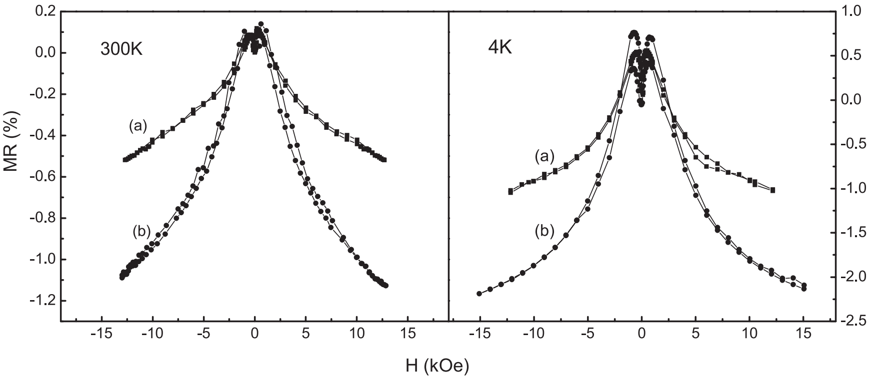

**Fig. 6.** Magnetoresistances versus applied field for the samples (a) $FeNi_3/Al_2O_3$-8, (b) $FeNi_3/Al_2O_3$-20 at room temperature and 4 K.

content of 20% (Al/(Fe+Ni)) is independent of frequency up to at least 1 GHz, and the imaginary part of the permeability is very small. The MR effects of $Al_2O_3/FeNi_3$ nanocomposites at low field could be related to TMR arising from the presence of insulating alumina shell and the AMR of Fe-Ni alloy core.

The author would like to thank Prof. Peter C.T. Au (Department of Chemistry, Hong Kong Baptist University) for valuable suggestions. This work was supported by the National Natural Science Foundation of China under Grant No. 50471049, Sino-Israeli joint research project and the National Key Project for Basic Research (No. G1999064508), China.

## References

1. V.M. Petrov, V.V. Gagulin, Inorg. Mater. **37**, 135 (2001)
2. F. Mazaleyrat, L.K. Varga, J. Magn. Magn. Mater. **215–216**, 253 (2000)
3. S. Ohnuma, H.J. Lee, N. Kobayashi, H. Fujimori, T. Masumoto, IEEE Trans. Magn. **37**, 2251 (2001)
4. S. Russek, P. Kabois, T. Silva, F.B. Mancoff, S.D. Wang, Z. Qian, J.M. Daughton, IEEE Trans. Magn. **37**, 2248 (2001)
5. S. Ohnuma, T. Masumoto, Acta Mater. **44**, 1309 (2001)
6. Y.W. Zhao, C.Y. Ni, D. Kruczynski, X.K. Zhang, J.Q. Xiao, J. Phys. Chem. B **108**, 3691 (2004)
7. S. Ohnuma, N. Kobayashi, T. Masumoto, S. Mitami, H. Fujimori, J. Appl. Phys. **85**, 4543 (1999)
8. K. Ikeda, N. Kobayashi, H. Fujimori, J. Appl. Phys. **92**, 5395 (2002)
9. A. Ya. Vovk, J.Q. Wang, A.M. Pogoriliy, O.V. Shypil, A.F. Kravets, J. Magn. Magn. Mater. **242–245**, 476 (2002)
10. M. Sharma, S.X. Wang, J.H. Nickel, Phys. Rev. Lett. **82**, 616 (1999)
11. M.Z. Wu, Y.D. Zhang, S. Hui, et al., J. Appl. Phys. **92**, 6809 (2002)
12. H. Fujimori, S. Mitani, S. Ohnuma, J. Magn. Magn. Mater. **156**, 311 (1996)
13. K. Yakushiji, S. Mitani, K. Takanashi et al., J. Magn. Magn. Mater. **212**, 75 (2000)